Talanta 246 (2022) 123502

Contents lists available at ScienceDirect

Talanta

journal homepage: www.elsevier.com/locate/talanta

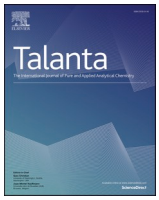

Isothermal amplification-mediated lateral flow biosensors for *in vitro* diagnosis of gastric cancer-related microRNAs

Seung Beom Seo [a,b], Jin-Seong Hwang [c,d], Eunjung Kim [e,f], Kyujung Kim [b], Seokbeom Roh [g,h], Gyudo Lee [g,h], Jaewoo Lim [a,i], Byunghoon Kang [a], Soojin Jang [a,i], Seong Uk Son [a,i], Taejoon Kang [a], Juyeon Jung [a], Jang-Seong Kim [c,d], Keun-Hur [j], Tae-Su Han [c,d,**], Eun-Kyung Lim [a,i,*]

[a] *Bionanotechnology Research Center, Korea Research Institute of Bioscience and Biotechnology (KRIBB), Daejeon, 34141, Republic of Korea*
[b] *Department of Cogno-Mechatronics Engineering, Pusan National University, Pusan, 46241, Republic of Korea*
[c] *Biotherapeutics Translational Research Center, KRIBB, Daejeon, 34141, Republic of Korea*
[d] *Department of Functional Genomics, KRIBB School of Biotechnology, University of Science and Technology (UST), Daejeon, 34113, Republic of Korea*
[e] *Department of Bioengineering & Nano-bioengineering, Incheon National University, Incheon, 22012, Republic of Korea*
[f] *Division of Bioengineering, Incheon National University, Incheon, 22012, Republic of Korea*
[g] *Department of Biotechnology and Bioinformatics, Korea University, Sejong, 30019, Republic of Korea*
[h] *Interdisciplinary Graduate Program for Artificial Intelligence Smart Convergence Technology, Korea University, Sejong, 30019, Republic of Korea*
[i] *Department of Nanobiotechnology, KRIBB School of Biotechnology, UST, Daejeon, 34113, Republic of Korea*
[j] *Department of Biochemistry and Cell Biology, School of Medicine, Kyungpook National University, Daegu, 41944, Republic of Korea*

ARTICLE INFO

Keywords:
Gastric cancer
microRNAs
Lateral flow biosensor
Rolling circle amplification
In vitro diagnosis

ABSTRACT

MicroRNAs (miRNAs) are important diagnostic and prognostic biomarkers for various tumors. Currently, many diagnostic systems have been developed to detect miRNAs, but simple techniques for detecting miRNAs are still required. Recently, we reported that the expression of miRNA-135b is upregulated in gastric epithelial cells during gastric inflammation and carcinogenesis. Our aim was to develop an *in vitro* diagnostic platform to analyze the expression of gastric cancer-related biomarkers in the blood. The diagnostic platform comprised an isothermal amplification-based lateral flow biosensor (IA-LFB) that enables easy diagnosis of gastric cancer through visual observation. In this platform, trace amounts of biomarkers are isothermally amplified through rolling circle amplification (RCA), and the amplified product is grafted to the LFB. The performance of the IA-LFB was confirmed using RNAs extracted from *in vitro* and *in vivo* models. The platform could detect target miRNAs within 3 h with excellent sensitivity and selectivity. In particular, the IA-LFB could detect the overexpression of gastric cancer-related markers (miRNA-135b and miRNA-21) in RNAs extracted from the blood of patients with various stages (stages 1–4) of gastric cancer compared to that in healthy volunteers. Therefore, IA-LFB is a simple and sensitive *in vitro* diagnostic system for detecting gastric cancer-related biomarkers and can contribute to the early diagnosis and prognosis monitoring of gastric cancer. Furthermore, this technology can be applied to systems that can detect multiple biomarkers related to various diseases (such as infectious and genetic diseases).

1. Introduction

Among the various types of cancers diagnosed worldwide, gastric cancer is common among both males and females. In 2018, an estimated 26,240 new cases of gastric cancer and 10,800 gastric cancer-related deaths were reported in the United States of America [1]. The incidence of gastric cancer is high among the Asian population, which accounts for approximately 75% of gastric cancer cases globally. Recently, liquid biopsy has emerged as an alternative to standard biopsy for the diagnosis of diseases, such as cancer [2,3]. *In vitro* diagnosis (IVD) and monitoring of cancer using body fluids have piqued the interest of the scientific community [4,5]. IVD is based on the detection of

* Corresponding author. Bionanotechnology Research Center, Korea research institute of bioscience and biotechnology (KRIBB), Daejeon, 34141, Republic of Korea.
** Corresponding author. Biotherapeutics Translational Research Center, KRIBB, Daejeon, 34141, Republic of Korea.
E-mail addresses: tshan@kribb.re.kr (T.-S. Han), eklim1112@kribb.re.kr (E.-K. Lim).

https://doi.org/10.1016/j.talanta.2022.123502
Received 15 February 2022; Received in revised form 18 April 2022; Accepted 22 April 2022
Available online 27 April 2022

nucleic acids derived from cancer cells in body fluids, which are obtained using a non-invasive liquid biopsy method. Body fluids comprise various biomarkers, such as proteins, DNAs, RNAs, and extracellular vesicles. RNA biomarkers include microRNAs (miRNAs), which are short non-coding endogenous RNAs with a length of 18–23 nucleotides. miRNAs regulate gene expression through translation inhibition or transcription repression by binding to the 3′-untranslated region (UTR) of the target transcript [6,7]. As miRNAs regulate genes associated with cell proliferation, differentiation, and apoptosis, they have been widely used as diagnostic and prognostic markers for cancer [8–11]. miRNA detection, which is universally used in clinical practice, is a molecular diagnostic technique based on DNA or RNA. Although northern blotting is associated with enhanced sensitivity for RNA detection, it is not suitable for analyzing clinical samples as it is a low-throughput technique and involves multiple steps [12,13]. Reverse transcription-loop-mediated isothermal amplification (RT-LAMP), which involves the amplification of genes through a substitution reaction, is a rapid diagnostic technique and does not require special equipment. However, the design of an RT-LAMP assay is challenging as it involves four primers [14,15]. Quantitative real-time polymerase chain reaction (qRT-PCR) has been widely applied to analyze clinical samples owing to its high sensitivity and accuracy but requires expensive equipment [16,17]. Lateral flow immunoassay (LFIA), which is a simple diagnostic method based on chromatography-like migration of a labeled target substance through multiple membranes, involves an antigen-antibody reaction to display a test line (TL) and a control line (CL) on the membrane to visually confirm the presence of a target substance [18–20]. The major advantage of LFIA is the easy interpretation of results through simple visualization without the need for additional analytical equipment [21]. LFIA has applications in immunodiagnosis to detect proteins such as antigens or antibodies. Recently, LFIA has also been used to detect genes [22–25]. However, the concentration of target genes in samples is generally too low for direct LFIA applications. Hence, LFIA must be combined with a molecular diagnostic technology to achieve sufficient detection sensitivity. Therefore, gene amplification technology has been used to increase detection sensitivity. In particular, amplifying genes under isothermal conditions is reported to be effective for IVD through point-of-care testing. Isothermal amplification improves detection sensitivity by amplifying trace genes without the need for expensive equipment and high analysis costs. The most common isothermal gene amplification techniques include strand displacement amplification, hybridized chain reaction (HCA) [26], and rolling circle amplification (RCA) [27,28]. RCA technology is based on the binding of a small amount of miRNA to a padlock probe [29–31], and the bound miRNAs are subsequently amplified into large amounts of DNA molecules. Thus, RCA technology has high sensitivity to detect a target. Recently, we had reported that the expression of miRNA-135b was upregulated in all gastric epithelial cell types after *Helicobacter felis* infection and that miRNA-135b and miRNA-21 were upregulated in gastric epithelial cells during gastric inflammation and carcinogenesis [32–34]. This study aimed to design a lateral flow-based biosensor (LFB) with RCA technology to enable simple and efficient detection of gastric cancer-related markers (miRNA-135b and miRNA-21).

2. Experimental section

2.1. Materials

All oligonucleotides, which were purchased from Bioneer Co. (Daejeon, Korea), were purified using high-performance liquid chromatography and dissolved in diethylpyrocarbonate (DEPC)-treated deionized water (DEPC water). CircLigase™ II ssDNA ligase (100 U/μL), CircLigase™ II 10 × reaction buffer, 50 mM $MnCl_2$, and 5 M betaine were purchased from Epicentre Biotechnologies Co. (Madison, WI, USA). Phi29 DNA polymerase, 10 × phi29 DNA polymerase buffer, exonuclease I, and diluent A were purchased from New England Biolabs Co. (Ipswich, MA, USA). Deoxynucleotide triphosphates (dNTPs) were purchased from TaKaRa Bio. Inc. (Shiga, Japan). Biosesang Co. (Seoul, Korea) provided 1 × Tris-EDTA (TE) buffer and Tris-borate-EDTA (TBE) buffer, while Costar Co. (Washington, USA) provided the 96-well solid black flat-bottom polystyrene TC-treated microplates. Milenia GenLine HybriDetect was purchased from Milenia Biotec Co. (Giessen, Germany). GelRed® nucleic acid stain was purchased from Biotium Co. (Fremont, CA, USA).

2.2. Designing probes for RCA

The capture probe has a complementary sequence that hybridizes with the 12-bp nucleotide sequence of the 23-bp target miRNA. The remaining 11 bp sequence of the target binds to the complementary sequence of the circular DNA (Table S1). The isothermal amplification reaction occurs at 37 °C within 2 h after hybridization. The secondary structures of the padlock probe and binding primers were analyzed using Nucleic Acid Package (NUPACK) software (http://www.nupack.org) (Fig. S1).

2.2.1. Circularization of the padlock probe

The linear RCA template (10 μmol/L) was circularized using CircLigase™ II ssDNA ligase at 60 °C for 16 h in a reaction buffer containing 10 × Circligase™ ssDNA ligase buffer, 2.5 mmol/L $MnCl_2$, 1 mol/L betaine, and ssDNA ligase (5 U/μL). Next, the enzyme was inactivated at 80 °C for 10 min. Un-circularized template was digested by incubating the samples with exonuclease I (10 U/μL) at 37 °C for 1 h. Enzyme inactivation was performed at 80 °C for 20 min. The resulting circular DNA was used without further purification. The final product of circularization reaction was confirmed by subjecting the samples to native polyacrylamide gel electrophoresis (PAGE) using a 10% gel.

2.3. miRNA amplification using RCA reaction

The ligation reaction was performed using a 20-μL reaction mixture comprising DEPC water, 2 μL of capture probe (1 μM), and various target miRNA concentrations at 37 °C for 30 min. The binding of target miRNA to circular DNA (10 μL) was facilitated by incubating the reaction mixture at 55 °C for 5 min, followed by immediate cooling to 37 °C for 1 h. The RCA reaction was performed at 37 °C in a final volume of 40 μL containing 1 × phi29 DNA polymerase buffer (50 mM Tris-HCl (pH 7.5), 10 mM $MgCl_2$, 10 mM $(NH_4)_2SO_4$, and 4 mM dithiothreitol), phi29 DNA polymerase (1 μL, 10 U/μL), and dNTPs (4 μL, each 2.5 mM) for 2 h. Enzyme inactivation was performed by incubating the reaction mixture at 65 °C for 10 min. The resulting mixture was incubated with the reporter probe (1 nM) at 37 °C for 30 min.

2.4. Electrophoresis and atomic force microscope (AFM) image analysis of RCA product

The RCA products were analyzed using native PAGE with a 10% gel. The composition of the reaction solution was 1 × phi29 DNA polymerase reaction buffer, phi29 DNA polymerase (10 U), dNTPs (each 2.5 mM), circular DNA (10 μL), capture probe (500 nM), and target DNA (500 nM). Next, 40 μL of each reaction product was electrophoresed in 1 × TBE buffer (running buffer) under a constant voltage of 80 V for 60 min. The gel was stained with GelRed® and scanned using an ultraviolet transilluminator (BioRad, California, USA). AFM analysis was performed with a Multimode 8 AFM (Bruker, USA) under ambient conditions using the AFM tips (PR-T300, Probes Inc.). Scanning was performed in the tapping mode. The data were analyzed with Nanoscope Analysis software. For the preparation of polylysine (PL)-coated mica, PL solution was prepared by dissolving L-lysine in distilled water (Gibco™). Next, the PL solution (1 mg/mL; 50 μL) was incubated on freshly cleaved mica for 1 min. The mica was rinsed with distilled water

and completely dried using an air gun. The PL-coated mica was used immediately to analyze RCA products. The scanning conditions were as follows: scan rate, 0.2 Hz; scan size, 2 × 2 μm^2.

2.5. miRNA detection using IA-LFB

For visual detection of gastric cancer-associated miRNAs (miRNA-135b and miRNA-21) using the HydriDetect lateral flow test strip, 45 μL of RCA product mixed with HydriDetect assay buffer was transferred to a 96-well plate (Costar, Washington, USA). Next, a dipstick was placed into each well, and the samples were incubated at room temperature for 15 min, followed by drying for an additional 15 min. The TL of IA-LFB was analyzed using a ChemiDoc™ MP imaging System with Image Lab (BioRad, California, USA).

2.6. Establishment of an in vitro model (miRNA-135b-expressing cancer cell line)

The detailed procedures for establishing an miRNA-135b-expressing cell line have been described elsewhere [34]. Briefly, the human gastric cancer cell line (SNU-638) obtained from the Korean Cell Line Bank (Seoul, Korea) was maintained in Roswell Park Memorial Institute medium (Welgene) supplemented with 10% fetal bovine serum and a 1% antibiotic-antimycotic solution. To establish a stable miRNA 135b-expressing cell line, the full-length coding region of miRNA-135b cDNA was amplified and cloned into the pmR-ZsGreen1 vector (Takara Bio Inc.). The following primers were used for miRNA-135b cloning: 5′-CCGCTCGAGTTTATGGCCAGGAAG-3′ (forward) and 5′-CGGGATCC AAGGTCTCCTTCCTT-3′ (reverse). To select the miRNA-135b-expressing cells (SNU-638 135b over), 500 μg/mL geneticin (Thermo Fisher Scientific) was added to the medium. Green fluorescence protein (GFP)-positive cells were sorted using a fluorescence-activated cell sorter (Thermo Fisher Scientific, Waltham, MA, USA).

2.7. Establishment of an in vivo model (gastric cancer xenograft model)

To establish a xenograft mouse model, the right flank of female Balb/c-nu mice (Orientibio, Seongnam, Korea) aged 5 weeks was subcutaneously injected with empty vector-transfected (SNU-638 control) or stable miRNA-135b-overexpressing SNU-638 cells (SNU-638 135b over). The tumor size was measured twice a week using calipers, and the tumor volume was calculated. The serum and tumor tissues from mice were collected for analysis. The animal experiments were approved by the Committee on Animal Experimentation of the Korea Research Institute of Bioscience and Biotechnology.

2.8. Clinical samples of gastric cancer

This study was approved by the Institutional Review Board of the Biobank of Ajou University Hospital and the Korea Research Institute of Bioscience and Biotechnology. In this study, 15 human serum samples (5 from healthy volunteers and 10 from patients with gastric cancer) were obtained from the Biobank of Ajou University Hospital.

2.9. Analysis of RNA expression in biological samples using qRT-PCR

Exosomes from human and mouse serum samples were isolated using ExoQuick™ (System Biosciences, Palo Alto, CA), while those from the cell culture medium were isolated using ExoQuic-TC™ (System Biosciences), following the manufacturer's instructions. Exosomal RNA was extracted using the RNeasy Micro kit (Qiagen). Total RNAs were isolated from cells (*in vitro* model) and mouse tumor tissues (*in vivo* model) using Nucleosol (Macherey-Nagel Co.). The isolated RNAs were reverse-transcribed into complementary DNA (cDNA). qRT-PCR analysis was performed an using HB miR Multi Assay kit™ System I (Heimbiotek, Seongnam, Korea) with StepOne Plus (Applied Biosystems). The PCR conditions were as follows: initial denaturation at 95 °C for 15 min, followed by 45 cycles at 95 °C for 10 s (denaturation) and 60 °C for 40 s (annealing/extension). The expression levels of miRNA-135b (target miRNA of gastric cancer) and miRNA-21 (oncogenic target miRNA) were analyzed using an HB miR Multi Assay kit™ System I and normalized to those of *RNU6B* (reference gene).

2.10. Statistical analysis

Data were obtained from at least three independent experiments. The exact number of replicates has been included in each graph. Data are represented as mean ± standard deviation of triplicate tests. The following legend has been added to the figures: $*p < 0.05$; $**p < 0.005$; and $***p < 0.00005$.

3. Results and discussion

3.1. Principle of miRNA detection using IA-LFB

An IA-LFB was developed to enable IVD of gastric cancer and monitoring of its progression through simple visualization. The IA-LFB was designed to detect specific gastric cancer-related miRNA biomarkers (miRNA-135b and miRNA-21). The process of isothermal amplification in RCA, which is illustrated in Scheme 1a, comprises the following three steps: binding of the capture probe to target miRNA; binding of the capture probe/miRNA complex to circular DNA; RCA of the target. After annealing of the detection probe to the RCA product, the LFB was incubated in a buffer containing the RCA product. The target miRNA in the sample binds to streptavidin on the TL of the dipstick and biotin on the capture probe in the RCA product. Additionally, the target miRNA binds to FAM of the detection probe and anti-fluorescein isothiocyanate antibody-modified gold particles. This sandwich binding results in the appearance of the TL. The appearance of the CL indicates the optimal performance of the dipstick (sample flow and the active state of the biomolecule [anti-FAM antibody] on the gold nanoparticles). Therefore, only the CL is observed in the absence of the target miRNA (Scheme 1b).

3.1.1. Design of RCA probes for gastric cancer-associated miRNA detection

We designed RCA-based probes (padlock and capture probes) that can promote the isothermal amplification of target miRNAs (miRNA-135b and miRNA-21). The sequences of the padlock and capture probes are listed in Table S1. The optimal sequences of probes were determined using the NUPACK software to avoid the formation of a secondary bond structure between the padlock probe and the capture probe and target miRNA sequence (Fig. S1). The sequence did not form self-secondary structures at the reaction temperature. The annealing of the capture probe with the target 21–23 bp of miR-135b and miR-21 was performed at 37 °C. Meanwhile, the annealing of the capture probe/target miRNA complex to the padlock probe was performed at 55 °C for 5 min, followed by incubation at 37 °C for 1 h. The bound circular template DNA was incubated at 37 °C with the RCA enzyme mixture. As shown in Fig. 1a, the samples were subjected to PAGE analysis, which revealed a combination of target-mediated probes and RCA reactants. Capture probes, target miRNAs (miRNA-135b and miRNA-21), and circular DNA were observed at approximately 25–27, 22–23, and 50 bp (Lanes 1–3), respectively. Lane 4 comprised the RCA product. In contrast to the size of the product in the other lanes, the size of the enzyme-dependent amplification product was too large to resolve in the gel. PAGE analysis revealed that the RCA product exhibited a band at the top of the gel, while the unamplified binding probe exhibited a weak band at the bottom of the gel. These findings indicate that the developed system works optimally and that sufficient signals are generated in the presence of target miRNAs. Additionally, the formation of the RCA product was confirmed by AFM images, which revealed the presence of linear single-stranded DNA with lengths in the micrometer range. The RCA products

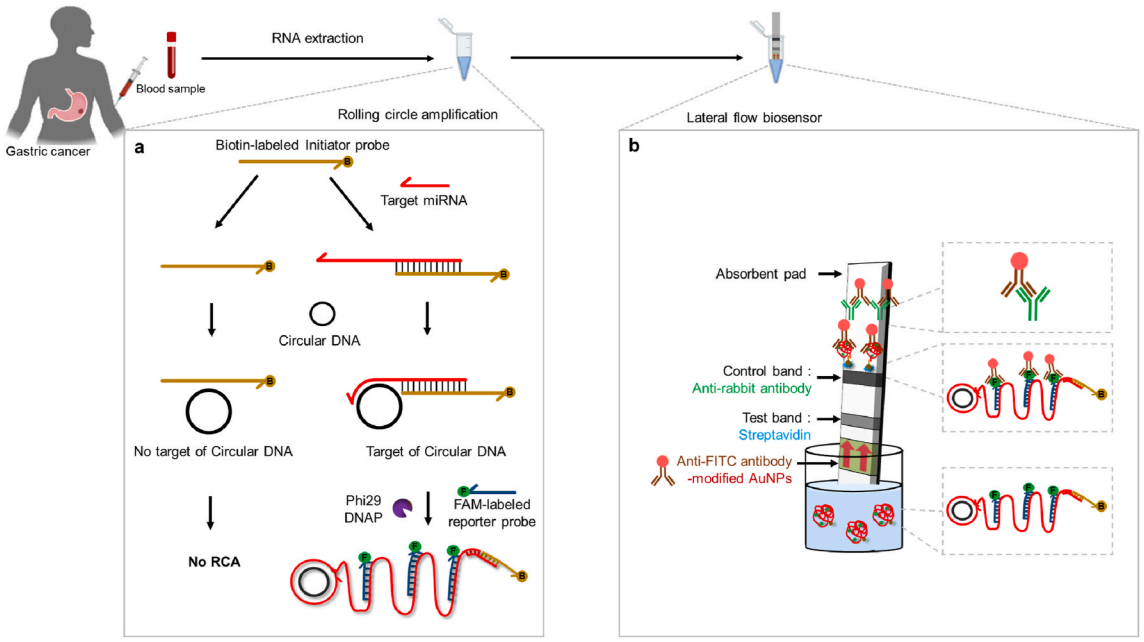

Scheme 1. Overview of the isothermal amplification-based lateral flow biosensor (IA-LFB). (a) Illustration of rolling circle amplification (RCA)-based isothermal amplification reaction for ultrasensitive microRNA (miRNA) detection in blood samples of patients with gastric cancer (B: biotin and F: FAM fluorescent dye). (b) The amplified RCA product of IA-LFB can bind to antibody-modified gold particles, and the target miRNA can be visually identified.

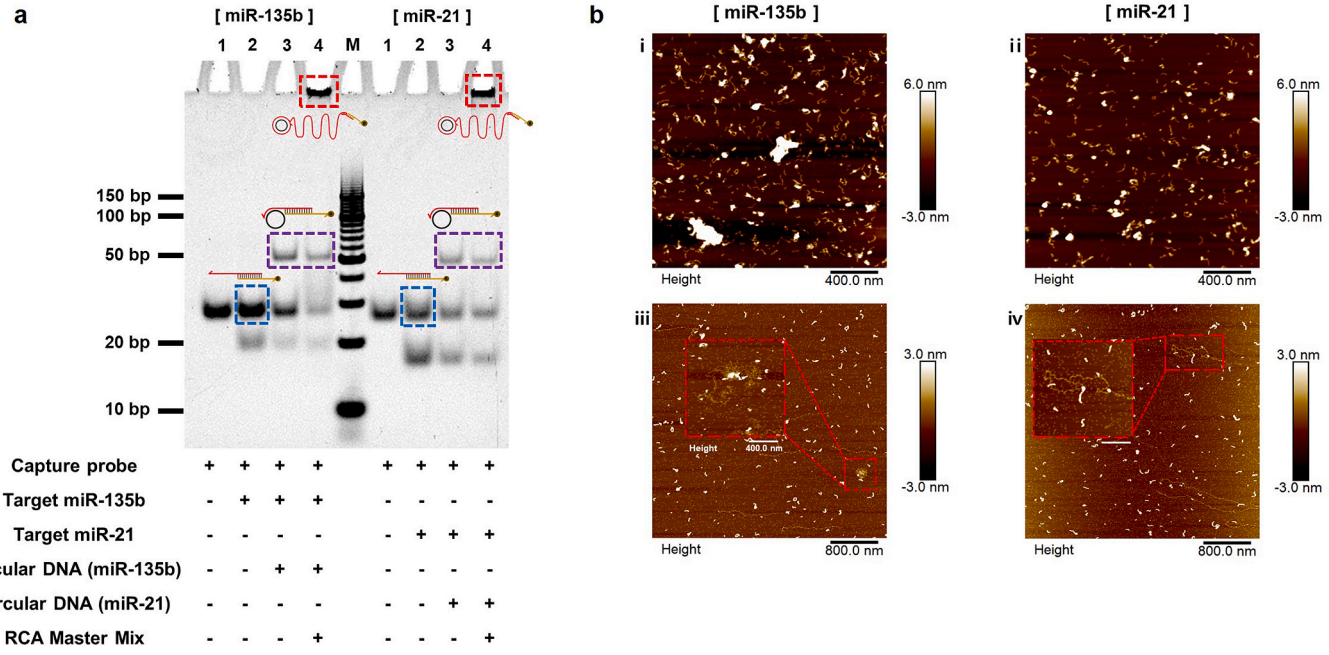

Fig. 1. Analysis of rolling circle amplification (RCA)-based isothermal microRNA (miRNA) amplification. (a) Evaluation of isothermal miRNA amplification products with RCA probes using a native polyacrylamide gel. Analysis of probe mixture separated based on size (left: miRNA-135b, right: miRNA-21). M, 10 bp DNA marker; lane 1, capture probe (CP); lane 2, the mixture of CP and target (T); lane 3, the mixture of CP, T, and circular DNA before RCA reaction; lane 4, the mixture of CP, T, and circular DNA after RCA reaction. (b) Atomic force microscopy (AFM) image of RCA product according to the presence of target miRNAs. (i and iii: high-magnification images after RCA reaction; ii and iv: low-magnification images after RCA reaction).

of the target miRNAs (miRNA-135b and miRNA-21) were confirmed in the AFM images (Fig. 1b). DNA molecules on mica exhibit a dense structure with different conformations, such as super twisting, base-paired single-stranded DNA molecules, and circular DNA conformations due to loop flexibility. In particular, circular DNA and unamplified short linear DNA were observed in the non-target control images (Fig. 1b i and iii), whereas long amplified DNA molecules were observed in the RCA product (Fig. 1b ii and iv). The control of the mica substrates reduced enzyme interference and allowed DNA molecules to spread uniformly, thereby obtaining a clean image of DNA molecules. These results demonstrate successful amplification of single-stranded DNA molecules from the 50-bp templates.

3.2. Performance (sensitivity and selectivity) evaluation of IA-LFB

To evaluate the performance of IA-LFB, the reaction was performed using various concentrations of RNAs containing target miRNAs (miRNA-135b and miRNA-21). First, amplification of the target miRNA was examined using SYBR Green I (Fig. S2). Before application to the LFB, the RCA product in the solution phase was identified using SYBR Green I. SYBR Green I intercalates with the RCA product to which the detection probe is bound and exhibits fluorescence. As shown in Fig. S2a–b, the fluorescence intensity gradually increased with the increase in target miRNA concentration. This indicated that the levels of the RCA product increased with the increase in target concentration. Additionally, analysis of the negative control revealed that the target DNA in the solution was amplified through specific bonds (Fig. S3a–b). The previously optimized RCA enzyme concentration was applied on a dipstick. To visualize this, an RCA product at an adjusted concentration was prepared and applied to LFB. Bands appeared in the TL and CL (Fig. 2a and c). The test concentration of the miRNA was in the range of 10 pM to 10 nM. The appearance of TL even at a low miRNA concentration indicates the high sensitivity of the sensor. The detection limit (limit of detection) of the sensor was 0.1 nM. Additionally, other miRNAs (miRNA-103-3p, miRNA-143-3p, miRNA-365-5p, miRNA-30e-5p, miRNA-342-3p, miRNA-574, and let-7i) were used as negative controls to confirm the selectivity of the sensor (Table S2). Each RCA probe set specifically bound and amplified only the target miRNA, which was verified both in the solution phase and the dipstick (Fig. 2b and d). miRNA-135b and miRNA-21, which are tumor-associated biomarkers, can both be present in clinical samples. Hence, there is a need to analyze the non-specific reaction between the circular DNA and the target miRNAs (Fig. S4a and b). Target miRNA cross-reactivity test was conducted using IA-LFB. The system could visually detect a low concentration of target miRNA with high sensitivity and excellent selectivity.

3.3. Detection of miRNA from in vitro samples using IA-LFB

SNU-638 cells exhibit downregulated expression of miRNA-135b, whereas SNU-638 135b over cells exhibit upregulated expression. The expression levels of miRNA-135b in SNU-638 135b over and SNU-638 cells were comparatively analyzed using qRT-PCR (Fig. S5a). Compared with those in SNU-638 cells, the expression levels of miRNA-135b were upregulated by more than 20-fold in SNU-638 135b over cells. Next, the performance of IA-LFB was evaluated using total RNAs extracted from SNU-638 and SNU-638 135b over cells. Various concentrations of RNAs (0.05–25 ng/reaction) were used for the RCA reaction, and the RCA products were applied to the IA-LFB. As shown in Fig. S5b, the TL was distinct when RNA samples extracted from SNU-638 135b over cells were applied to the IA-LFB. In contrast, a weak TL was observed when RNA samples from SNU-638 cells were applied to IA-LFB. The intensity of the TL, which was analyzed using the ChemiDoc imaging systems, was directly proportional to the RNA concentrations. The TL intensity on IA-LFBs with RNA samples from SNU-638 135b over cells was higher compared to that on IA-LFBs with RNA samples extracted from control

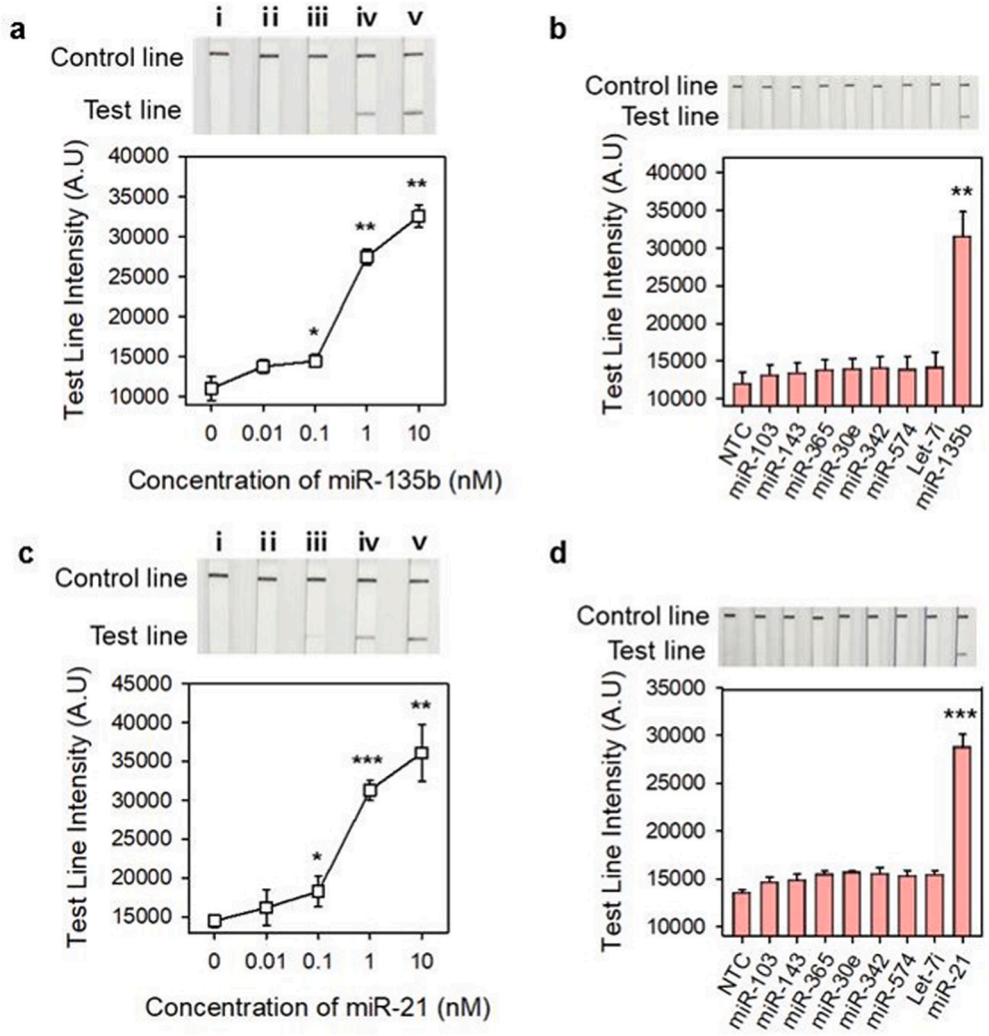

Fig. 2. Evaluation of the microRNA (miRNA) detection ability of an isothermal amplification-based lateral flow biosensor (IA-LFB). (a, c) Images of IA-LFB after application of various concentrations (or types) of RNAs to detect specific miRNAs and the intensities of each test line (a: miRNA-135b and c: miRNA-21). The concentrations of target miRNAs used for the analysis were (i) 0, (ii) 0.01, (iii) 0.1, (iv) 1, and (v) 10 nM. (b and d) Eight types of miRNAs were used as negative controls to confirm the selectivity of target miRNA detection (b: IA-LFB for miRNA-135b detection and d: IA-FB for miRNA-21 detection). NTC, no template control.

SNU-638 cells (Fig. S5c). In particular, the TL was distinct when RNA samples were applied at a concentration of 2.5 ng/reaction. The appearance of the CL was observed in all cases, which indicated the optimal performance of the system. Fig. S5d shows the heatmap of the TL intensity value of cellular miRNAs in RNA samples analyzed at concentrations of 0.05–25 ng per reaction. The TL intensity in IA-LFBs analyzing RNA samples from SNU-638 135b over cells was significantly higher compared to that in IA-LFBs analyzing RNA samples from SNU-638 control cells. The expression of the oncogenic miRNA-21 was similar in both SNU-638 and SNU-638 over cells, and the relative expression level was calculated as 1 (Fig. S6a). RNA extracted from control SNU-638 cells was applied to an IA-LFB to detect miRNA-21. The results indicated that the miRNA-21 TL intensity was directly proportional to the concentration of RNA used for the analysis. In particular, the TL was distinct when the RNA sample was applied at a concentration of 2.5 ng per reaction (Fig. S6b and c). To apply this system as a novel tool to analyze liquid biopsy samples in the field of precision cancer medicine, exosomal RNAs must be analyzed. Exosomes are small nano-sized vesicles released from cells and are generally stable in various body fluids [35]. Exosomes released from tumor cells are important biomarkers for cancer diagnosis and treatment because they contain nucleic acids and proteins that provide useful information on tumors [36,37]. The miRNA expression levels in the exosomes extracted from SNU-639 and SNU-638-miRNA-135b over cells were analyzed using qRT-PCR. Compared with those in the exosomes of SNU-638 cells, miRNA-135b levels were upregulated by more than 30-fold in the exosomes of SNU-638 135b over cells (Fig. 3a). Next, various concentrations of exosomal RNAs (0.05–5 ng per reaction) extracted from *in vitro* samples were applied to IA-LFB. The appearance timing (Fig. 3b) and intensity (Fig. 3c) of the TL in IA-LFBs exposed to exosomal RNAs from SNU-638 135b over cells were directly proportional to the concentration of RNA used for the analysis. In particular, the application of RNA samples (at concentrations $\geq$2.5 ng per reaction) from SNU-638 135b over cells resulted in the appearance of a distinct TL (Fig. 3b and d). Thus, the expression of exosomal RNA could be visually confirmed. Consistent with the results of cellular RNA analysis, the expression level of miRNA-21 in the exosomes was confirmed (Fig. S6d). The appearance timing and intensity of the miRNA-21 TL were directly proportional to the concentrations of RNA used for the analysis (Fig. S6e and S6f). These findings indicate that IA-LFB enables simple visual detection of cellular and exosomal RNAs.

3.4. Detection of miRNAs extracted from in vivo models using IA-LFB

Gastric cancer *in vivo* models were established by injecting SNU-638 135b over cells into the proximal thigh region of mice (n = 5). The

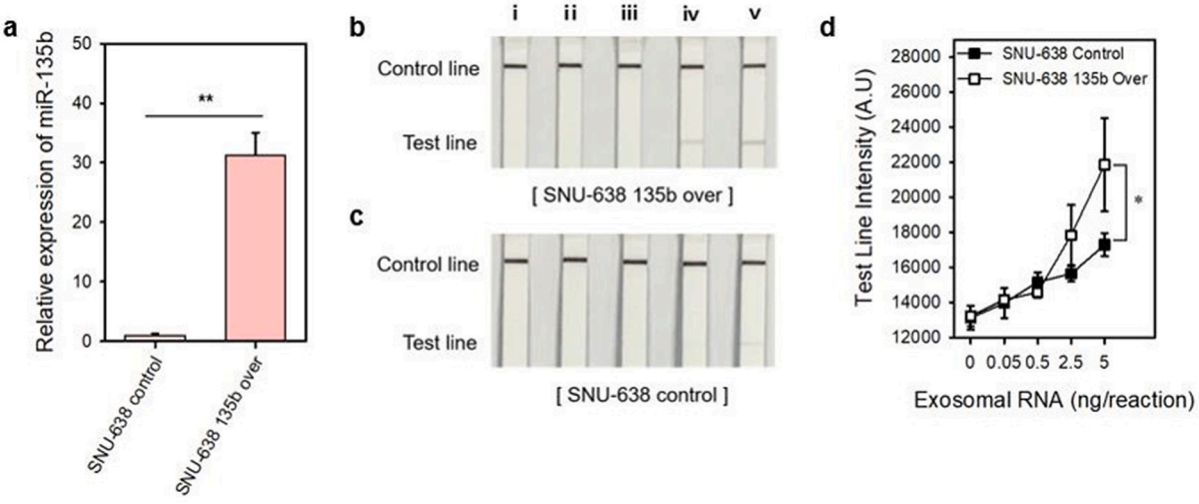

e

	ng/reaction	NTC	0.05	0.5	2.5	5
[SNU-638 control]	N = 1	13883	14749	15157	15434	17017
	N = 2	12671	14075	15702	16140	16803
	N = 3	12781	13042	14646	15321	18030
[SNU-638 135b over]	N = 1	13883	14440	14515	17084	22020
	N = 2	12796	13999	14928	16602	19121
	N = 3	12987	13978	14281	19803	24419

Fig. 3. Evaluation of the sensitivity of isothermal amplification-based lateral flow biosensor (IA-LFB) to detect miRNA-135b in exosomal RNA samples obtained from SNU-638 cells. (a) Comparative analysis of the relative expression levels of miRNA-135b in miRNA-135b-overexpressing SNU-638 (SNU-638 135b over) and control SNU-638 cells using quantitative real-time polymerase chain reaction. (b and c) The concentrations of exosomal RNA used for the analysis were (i) 0, (ii) 0.05, (iii) 0.5, (iv) 2.5, and (v) 5 ng per reaction. NTC, no template control. (d) A heatmap of the test line intensity values after the application of different concentrations of exosomal RNAs obtained from SNU-638 135b over and control SNU-638 cells.

control group was injected with control SNU-638 cells. On day 58 post-injection, xenograft mouse models were sacrificed, and the tumor tissues were excised. Tumor tissues of similar size were used for analysis (Fig. 4a), and each tumor was weighed (Fig. S7). The expression of miRNA-135b in the SNU-638 135b over cell-derived tumors was upregulated by approximately 10-fold when compared with that in the control SNU-638 cell-derived tumors (Fig. 4b). Additionally, the expression levels of miRNA-21 were similar between the control SNU-638 cell-derived and SNU-638 135b over cell-derived tumors (Fig. S8a). Next, RNA samples extracted from the tumor tissues were applied to IA-LFBs. The timing of TL appearance in the IA-LFBs was directly proportional to the RNA concentrations. The TLs were distinct when RNA samples from SNU-638 135b over cell-derived tumors were applied to IA-LFBs (Fig. 4d). Additionally, the TL intensity in IA-LFBs analyzing RNA samples from SNU-638 135b over cell-derived tumors was higher than that in IA-LFBs analyzing RNA samples from control SNU-638 cell-derived tumors (Fig. 4c and e). In contrast, the TL intensity was low in IA-LFBs analyzing RNA samples from control SNU-638 cell-derived tumors (Fig. 4c–**d**). The CLs were visible in all cases, which indicated the optimal performance of the system. The presence of miRNA-21 in the RNA samples of control SNU-638 cell-derived tumors was also visually confirmed using IA-LFBs (n = 5) (Fig. S8).

3.5. *Detection of miRNAs in the blood of patients with gastric cancer using IA-LFB*

The performance of the IA-LFB in detecting target miRNAs (miRNA-135b and miRNA-21) in the blood of patients with gastric cancer was examined. In total, 15 blood samples (5 from healthy volunteers, 5 from patients with stages I–II gastric cancer, and 5 from patients with stages III–IV gastric cancer) provided by the Biobank of Ajou University Hospital were used for the analysis. Total RNAs were isolated from the blood

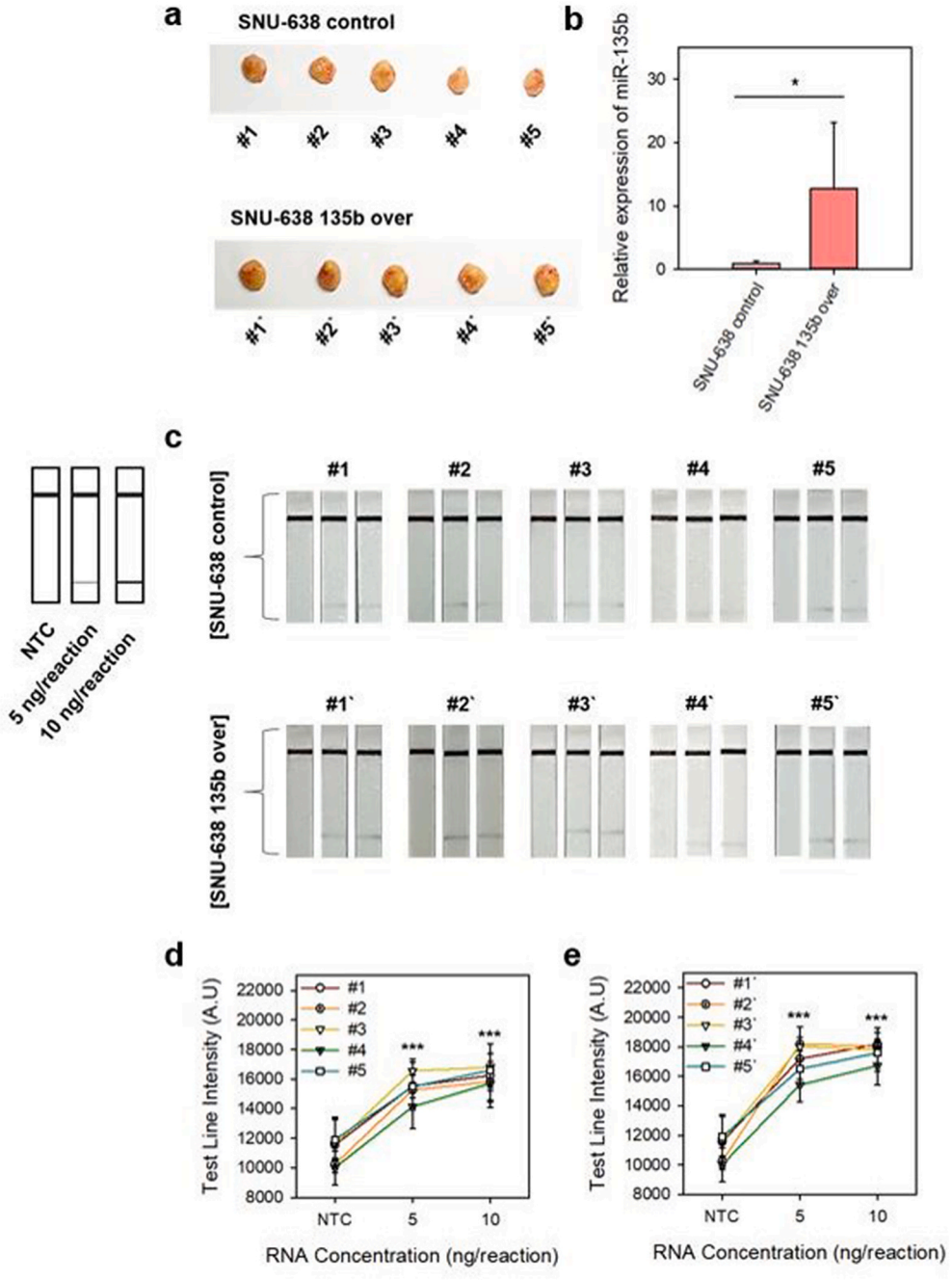

Fig. 4. Evaluation of the ability of isothermal amplification-based lateral flow biosensor (IA-LFB) to detect miRNA-135b in RNA samples extracted from *in vivo* models. (a) The images of excised tumors from mice injected with control SNU-638 (n = 5) and miRNA-135b-overexpressing SNU-638 cells (SNU-638 135b over cells) (n = 5). (b) Comparative analysis of the relative expression level of miRNA-135b in tumors using quantitative real-time polymerase chain reaction. (c–e) The ability of IA-LFB to detect miRNA-135b in RNA samples extracted from *in vivo* models (#1–#5, control SNU-638 cell-derived tumors; #1'–#5', SNU-638 135b over cell-derived tumors). The RNA concentrations used for the analysis were 0, 5, and 10 ng per reaction. NTC, no template control.

samples. The expression level of miRNA-135b in the blood of patients with gastric cancer and healthy volunteers was comparatively analyzed using qRT-PCR. The expression of miRNA-135b in the blood of patients with gastric cancer was upregulated by more than 4-fold when compared with that in the blood of healthy volunteers (Fig. 5a and b). Next, the ability of the IA-LFB to detect the target miRNAs in the blood samples was examined. As shown in Fig. 5c, the TL was observed when the RNA samples from patients with gastric cancer were applied to IA-LFBs. In contrast, TLs were not observed when RNA samples from healthy volunteers were applied to IA-LFBs. The TL appeared to be similar when RNA samples from healthy volunteers and patients with gastric cancer were applied to IA-LFBs. However, the TL intensity value in IA-LFBs analyzing RNA samples from patients with gastric cancer was higher compared to that in IA-LFBs analyzing RNA samples from healthy volunteers (Fig. 5d). Heatmap analysis revealed that the intensity of TL increases with the progression of cancer (Fig. 5e). These results demonstrated that the IA-LFB can diagnose gastric cancer from body fluids, such as blood, through simple visualization. Additionally, the IA-LFB could quantitatively analyze the differential expression of gastric cancer-related biomarkers (miRNAs) according to the stages of cancer progression.

4. Conclusions

We have developed an IA-LFB for the diagnosis of gastric cancer using body fluids, especially the blood. The incidence of gastric cancer is increasing worldwide. A recent study reported that miRNA-135b is a biomarker for gastric cancer caused by gastritis. In the diagnostic platform developed in this study, isothermally amplified miRNAs are applied to an IA-LFB. This platform enables the visual determination of the expression of target miRNAs in the form of a TL. The system can detect target miRNAs in a short duration (<3 h) under isothermal conditions. The performance of the system was verified using *in vitro/in vivo* samples, as well as using blood samples from patients with gastric cancer. Thus, specific biomarkers (miRNAs) expressed in cancers can be detected with an IA-LFB. These findings indicate the potential of IA-LFBs as an IVD tool for diagnosing cancer occurrence and monitoring its progression.

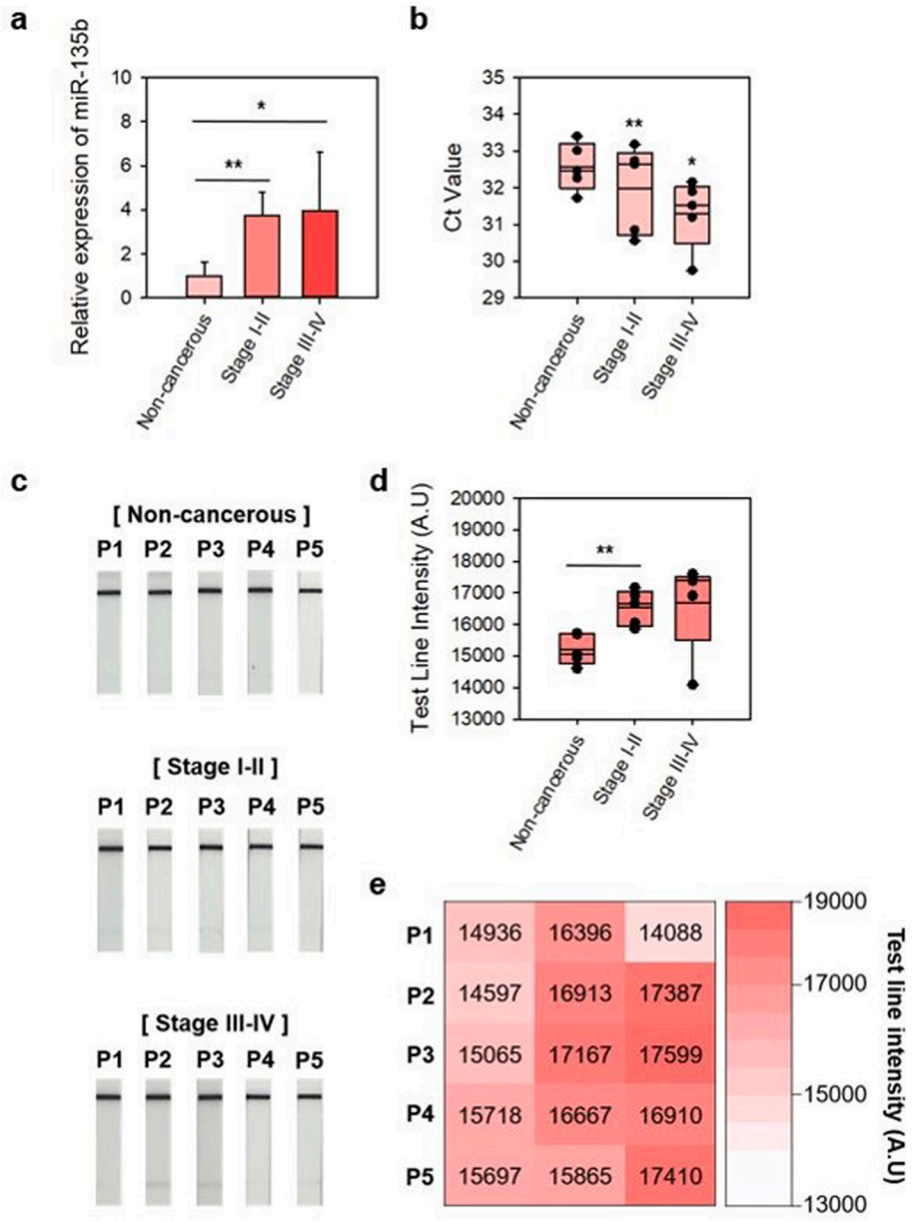

Fig. 5. Evaluating the performance of the isothermal amplification-based lateral flow biosensor (IA-LFB) using clinical samples. (a and b) Quantitative real-time polymerase chain reaction analysis of the relative expression levels of miRNA-135b in clinical samples. Ability of an IA-LFB to detect miRNA-135b in clinical samples. (c) Images of IA-LFBs after detection of miRNA-135b in RNA samples isolated from the blood of patients with various stages of gastric cancer (Stages I–II and Stages III–IV). (d) Test line intensities (circle: the intensity of the test line for each patient and bar: average and standard deviation). (e) A heatmap of the test line intensity values (d). P1–P5 indicates the number of patients.

Credit author statement

Seung Beom Seo: Conceptualization, Investigation, Data analysis, Writing – original draft preparation. **Jin-Seong Hwang**: Methodology, Investigation. **Eunjung Kim**: Writing- Review and editing. **Kyujung Kim**: Writing- Review and editing. **Seokbeom Roh**: Investigation. **Gyudo Lee**: Investigation. **Jaewoo Lim**: Data analysis. **Byunghoon Kang**: Data analysis. **Soojin Jang**: Data analysis. **Seong Uk Son**: Data analysis. **Taejoon Kang**: Writing- Review and editing. **Juyeon Jung**: Writing- Review and editing. **Jang-Seong Kim**: Writing- Review and editing. **Keun-Hur**: Resources. **Tae-Su Han**: Supervision, Methodology, Funding acquisition. **Eun-Kyung Lim**: Conceptualization, Supervision, Writing – original draft preparation, Funding acquisition.

Declaration of competing interest

The authors declare that they have no known competing financial interests or personal relationships that could have appeared to influence the work reported in this paper.

Acknowledgments

This research was supported by National R&D Programs through the National Research Foundation (NRF) of Korea funded by the Ministry of Science and ICT (MSIT) of Korea (NRF-2021M3E5E3080379, NRF-2021M3H4A1A02051048, NRF-2018M3A9E2022821, NRF-2021M3E5E3080844, NRF-2022R1C1C1008815, and NRF-2020R1A2C1010453), the Korean Fund for Regenerative Medicine (KFRM) grant funded by the Korean government (the Ministry of Science and ICT, the Ministry of Health & Welfare, 21A0404L1), the Technology Development Program for Biological Hazards Management in Indoor Air through the Korea Environment Industry & Technology Institute (KEITI) funded by the Ministry of Environment (ME) of Korea (2021003370003), the Industrial Strategic Technology Development Program (20009121) funded by the Ministry of Trade, Industry & Energy (MOTIE) of Korea, the Nanomedical Devices Development Program of National Nano Fab Center (CSM2105M101), and the KRIBB Research Initiative Program (1711134081 and 1711134038).

Appendix A. Supplementary data

Supplementary data to this article can be found online at https://doi.org/10.1016/j.talanta.2022.123502.

References

[1] R.L. Siegel, K.D. Miller, A. Jemal, Cancer statistics, 2018, CA. Cancer J. Clin. 68 (2018) 7–30, https://doi.org/10.3322/caac.21442.
[2] R. Palmirotta, D. Lovero, P. Cafforio, C. Felici, F. Mannavola, E. Pellè, D. Quaresmini, M. Tucci, F. Silvestris, Liquid biopsy of cancer: a multimodal diagnostic tool in clinical oncology, Ther. Adv. Med. Oncol. 10 (2018), https://doi.org/10.1177/1758835918794630.
[3] M. Antunes-Ferreira, D. Koppers-Lalic, T. Würdinger, Circulating platelets as liquid biopsy sources for cancer detection, Mol. Oncol. 15 (2021) 1727–1743, https://doi.org/10.1002/1878-0261.12859.
[4] J. Lim, B. Kang, H.Y. Son, B. Mun, Y.M. Huh, H.W. Rho, T. Kang, J. Moon, J.J. Lee, S.B. Seo, S. Jang, S.U. Son, J. Jung, S. Haam, E.K. Lim, Microfluidic device for one-step detection of breast cancer-derived exosomal mRNA in blood using signal-amplifiable 3D nanostructure, Biosens. Bioelectron. 197 (2022), https://doi.org/10.1016/j.bios.2021.113753.
[5] J. Moon, J. Lim, S. Lee, H.Y. Son, H.W. Rho, H. Kim, H. Kang, J. Jeong, E.K. Lim, J. Jung, Y.M. Huh, H.G. Park, T. Kang, Urinary exosomal mRNA detection using novel isothermal gene amplification method based on three-way junction, Biosens. Bioelectron. 167 (2020), https://doi.org/10.1016/j.bios.2020.112474.
[6] M. Ha, V.N. Kim, Regulation of microRNA biogenesis, Nat. Rev. Mol. Cell Biol. 15 (2014) 509–524, https://doi.org/10.1038/nrm3838.
[7] D. Vasilatou, S. Papageorgiou, V. Pappa, E. Papageorgiou, J. Dervenoulas, The role of microRNAs in normal and malignant hematopoiesis, Eur. J. Haematol. 84 (2010) 1–16, https://doi.org/10.1111/j.1600-0609.2009.01348.x.
[8] S. Lin, R.I. Gregory, MicroRNA biogenesis pathways in cancer, Nat. Rev. Cancer 15 (2015) 321–333, https://doi.org/10.1038/nrc3932.
[9] M.J. Bueno, I.P. De Castro, M. Malumbres, Control of cell proliferation pathways by microRNAs, Cell Cycle 7 (2008) 3143–3148, https://doi.org/10.4161/cc.7.20.6833.
[10] X. Chen, Y. Ba, L. Ma, X. Cai, Y. Yin, K. Wang, J. Guo, Y. Zhang, J. Chen, X. Guo, Q. Li, X. Li, W. Wang, Y. Zhang, J. Wang, X. Jiang, Y. Xiang, C. Xu, P. Zheng, J. Zhang, R. Li, H. Zhang, X. Shang, T. Gong, G. Ning, J. Wang, K. Zen, J. Zhang, C. Y. Zhang, Characterization of microRNAs in serum: a novel class of biomarkers for diagnosis of cancer and other diseases, Cell Res. 18 (2008) 997–1006, https://doi.org/10.1038/cr.2008.282.
[11] Q. Wang, K. Xu, Y. Tong, X. Dai, T. Xu, D. He, J. Ying, Novel miRNA markers for the diagnosis and prognosis of endometrial cancer, J. Cell Mol. Med. 24 (2020) 4533–4546, https://doi.org/10.1111/jcmm.15111.
[12] S. Dangwal, C. Bang, T. Thum, Novel techniques and targets in cardiovascular microRNA research, Cardiovasc. Res. 93 (2012) 545–554, https://doi.org/10.1093/cvr/cvr297.
[13] G.S. Pall, A.J. Hamilton, Improved northern blot method for enhanced detection of small RNA, Nat. Protoc. 3 (2008) 1077–1084, https://doi.org/10.1038/nprot.2008.67.
[14] C. Li, Z. Li, H. Jia, J. Yan, One-step ultrasensitive detection of microRNAs with loop-mediated isothermal amplification (LAMP), Chem. Commun. 47 (2011) 2595–2597, https://doi.org/10.1039/c0cc03957h.
[15] M. Jiang, W. Pan, A. Arasthfer, W. Fang, L. Ling, H. Fang, F. Daneshnia, J. Yu, W. Liao, H. Pei, X. Li, C. Lass-Flörl, Development and validation of a rapid, single-step reverse transcriptase loop-mediated isothermal amplification (RT-LAMP) system potentially to Be used for reliable and high-throughput screening of COVID-19, Front. Cell. Infect. Microbiol. 10 (2020), https://doi.org/10.3389/fcimb.2020.00331.
[16] Q. Huang, L. Zheng, Y. Zhu, J. Zhang, H. Wen, J. Huang, J. Niu, X. Zhao, Q. Li, Multicolor combinatorial probe Coding for real-time PCR, PLoS One 6 (2011), https://doi.org/10.1371/journal.pone.0016033.
[17] C.B.F. Vogels, A.F. Brito, A.L. Wyllie, J.R. Fauver, I.M. Ott, C.C. Kalinich, M. E. Petrone, A. Casanovas-Massana, M. Catherine Muenker, A.J. Moore, J. Klein, P. Lu, A. Lu-Culligan, X. Jiang, D.J. Kim, E. Kudo, T. Mao, M. Moriyama, J.E. Oh, A. Park, J. Silva, E. Song, T. Takahashi, M. Taura, M. Tokuyama, A. Venkataraman, O. El Weizman, P. Wong, Y. Yang, N.R. Cheemarla, E.B. White, S. Lapidus, R. Earnest, B. Geng, P. Vijayakumar, C. Odio, J. Fournier, S. Bermejo, S. Farhadian, C.S. Dela Cruz, A. Iwasaki, A.I. Ko, M.L. Landry, E.F. Foxman, N.D. Grubaugh, Analytical sensitivity and efficiency comparisons of SARS-CoV-2 RT–qPCR primer–probe sets, Nat. Microbiol. 5 (2020) 1299–1305, https://doi.org/10.1038/s41564-020-0761-6.
[18] J.P. Broughton, X. Deng, G. Yu, C.L. Fasching, V. Servellita, J. Singh, X. Miao, J. A. Streithorst, A. Granados, A. Sotomayor-Gonzalez, K. Zorn, A. Gopez, E. Hsu, W. Gu, S. Miller, C.Y. Pan, H. Guevara, D.A. Wadford, J.S. Chen, C.Y. Chiu, CRISPR–Cas12-based detection of SARS-CoV-2, Nat. Biotechnol. 38 (2020) 870–874, https://doi.org/10.1038/s41587-020-0513-4.
[19] E. Xiong, L. Jiang, T. Tian, M. Hu, H. Yue, M. Huang, W. Lin, Y. Jiang, D. Zhu, X. Zhou, Simultaneous dual-gene diagnosis of SARS-CoV-2 based on CRISPR/Cas9-Mediated lateral flow assay, Angew. Chem. Int. Ed. 60 (2021) 5307–5315, https://doi.org/10.1002/anie.202014506.
[20] C. Zheng, K. Wang, W. Zheng, Y. Cheng, T. Li, B. Cao, Q. Jin, D. Cui, Rapid developments in lateral flow immunoassay for nucleic acid detection, Analyst 146 (2021) 1514–1528, https://doi.org/10.1039/d0an02150d.
[21] D.V. Sotnikov, A.V. Zherdev, B.B. Dzantiev, Lateral flow serodiagnosis in the double-antigen sandwich format: theoretical consideration and confirmation of advantages, Sensors (Switzerland) 21 (2021) 1–16, https://doi.org/10.3390/s21010039.
[22] X. Fu, J. Wen, J. Li, H. Lin, Y. Liu, X. Zhuang, C. Tian, L. Chen, Highly sensitive detection of prostate cancer specific PCA3 mimic DNA using SERS-based competitive lateral flow assay, Nanoscale 11 (2019) 15530–15536, https://doi.org/10.1039/c9nr04864b.
[23] X. Cao, Y. Sun, Y. Mao, M. Ran, Y. Liu, D. Lu, C. Bi, Rapid and sensitive detection of dual lung cancer-associated miRNA biomarkers by a novel SERS-LFA strip coupling with catalytic hairpin assembly signal amplification, J. Mater. Chem. C. 9 (2021) 3661–3671, https://doi.org/10.1039/d0tc05737a.
[24] J.S. Gootenberg, O.O. Abudayyeh, J.W. Lee, P. Essletzbichler, A.J. Dy, J. Joung, V. Verdine, N. Donghia, N.M. Daringer, C.A. Freije, C. Myhrvold, R.P. Bhattacharyya, J. Livny, A. Regev, E. V Koonin, D.T. Hung, P.C. Sabeti, J.J. Collins, † Feng Zhang, CRISPR TECHNOLOGY Nucleic acid detection with CRISPR-Cas13a/C2c2, n.d. https://www.science.org.
[25] J.S. Gootenberg, O.O. Abudayyeh, M.J. Kellner, J. Joung, J.J. Collins, F. Zhang, Multiplexed and portable nucleic acid detection platform with Cas13, Cas12a, and Csm6, n.d. https://www.science.org.
[26] Research highlights. http://www.nature.com/naturemethods, 2004.
[27] M.G. Mohsen, E.T. Kool, The discovery of rolling circle amplification and rolling circle transcription, Acc. Chem. Res. 49 (2016) 2540–2550, https://doi.org/10.1021/acs.accounts.6b00417.
[28] L. Gu, W. Yan, L. Liu, S. Wang, X. Zhang, M. Lyu, Research progress on rolling circle amplification (Rca)-based biomedical sensing, Pharmaceuticals 11 (2018), https://doi.org/10.3390/ph11020035.
[29] Q. Yao, Y. Wang, J. Wang, S. Chen, H. Liu, Z. Jiang, X. Zhang, S. Liu, Q. Yuan, X. Zhou, An ultrasensitive diagnostic biochip based on biomimetic periodic nanostructure-assisted rolling circle amplification, ACS Nano 12 (2018) 6777–6783, https://doi.org/10.1021/acsnano.8b01950.
[30] H. Liu, L. Li, L. Duan, X. Wang, Y. Xie, L. Tong, Q. Wang, B. Tang, High specific and ultrasensitive isothermal detection of microRNA by padlock probe-based

exponential rolling circle amplification, Anal. Chem. 85 (2013) 7941–7947, https://doi.org/10.1021/ac401715k.
[31] Q. Ma, P. Li, Z. Gao, S.F. Yau Li, Rapid, sensitive and highly specific label-free fluorescence biosensor for microRNA by branched rolling circle amplification, Sensor. Actuator. B Chem. 281 (2019) 424–431, https://doi.org/10.1016/j.snb.2018.10.141.
[32] M.L. Si, S. Zhu, H. Wu, Z. Lu, F. Wu, Y.Y. Mo, miR-21-mediated tumor growth, Oncogene 26 (2007) 2799–2803, https://doi.org/10.1038/sj.onc.1210083.
[33] D. Sekar, R. Krishnan, K. Thirugnanasambantham, B. Rajasekaran, V.I.H. Islam, P. Sekar, Significance of microRNA 21 in gastric cancer, Clin. Res. Hepatol. Gastroenterol. 40 (2016) 538–545, https://doi.org/10.1016/j.clinre.2016.02.010.
[34] T.S. Han, D.C.C. Voon, H. Oshima, M. Nakayama, K. Echizen, E. Sakai, Z.W. E. Yong, K. Murakami, L. Yu, T. Minamoto, C.Y. Ock, B.J. Jenkins, S.J. Kim, H. K. Yang, M. Oshima, Interleukin 1 up-regulates MicroRNA 135b to promote inflammation-associated gastric carcinogenesis in mice, Gastroenterology 156 (2019) 1140–1155, https://doi.org/10.1053/j.gastro.2018.11.059, e4.
[35] D.M. Pegtel, S.J. Gould, Annual Review of biochemistry exosomes. https://doi.org/10.1146/annurev-biochem-013118, 2019.
[36] S. Samanta, S. Rajasingh, N. Drosos, Z. Zhou, B. Dawn, J. Rajasingh, Exosomes: new molecular targets of diseases, Acta Pharmacol. Sin. 39 (2018) 501–513, https://doi.org/10.1038/aps.2017.162.
[37] I. Li, B.Y. Nabet, Exosomes in the tumor microenvironment as mediators of cancer therapy resistance, Mol. Cancer 18 (2019), https://doi.org/10.1186/s12943-019-0975-5.